Application of Energyflo® Dynamic Insulation in SAP Appendix Q

Introduction

This document provides the technical information and guidance required for Energyflo® dynamic insulation products to be assessed within SAP Appendix Q. It provides a brief overview of two types of dynamic insulation, the analytical equations that describe their performance and the validation of these equations against empirical data from a series of Modified Hot Box Tests of the products by the National Physical Laboratory (NPL).

Documents detailing the analytical models, copies of NPL reports and the SAP Appendix Q Effective U-value calculation spreadsheet that embodies these models are bundled as part of the proposed calculation method.

Working Principles of Dynamic Insulation

Dynamic insulation offers a new, energy-efficient approach to thermal insulation that can be used instead of, or in tandem with, conventional 'static' insulation in buildings. An important property of dynamic insulation is that it is permeable to air flow. This enables fresh ventilation air to be drawn into the building via appropriate inlet and outlet vents in the external fabric. As the air flows inwards through the dynamic insulation layer it is pre-tempered using the waste heat normally lost through the fabric of the building. Depending on the rate of air flow, part or all of the fabric heat that is normally lost is recovered to the building's fresh air ventilation supply.

Heat flow through a dynamically insulated wall (henceforth read to mean wall, roof, ceiling or floor) is conceptually simple to understand. Figure 1(a) shows the heat loss (A) through a conventionally insulated wall. Under steady state conditions and ignoring inertial effects (i.e., thermal mass), (A) is the same entering as leaving the wall, its magnitude determined by the resistance to heat flow of the materials used to build the wall. Figure 1(b) shows a dynamically insulated wall, where cold outdoor air is drawn in through the dynamic insulation layer and pre-heated by the heat loss (B), recovering part of that heat loss (C) to the building as pre-tempered air. The balance (D), which is the difference between (B) and (C), is what is lost from the building.

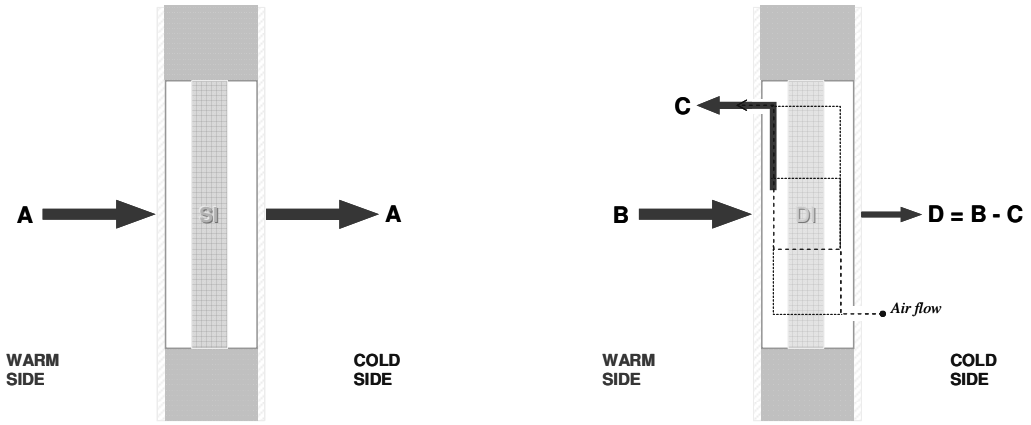

(a) Static wall construction (b) Dynamic wall construction

Figure 1

In the absence of air flow, a dynamically insulated wall should transmit heat in exactly the same way as the static wall – i.e., C = 0 and D = B. As air begins to flow inwards, the

net fabric heat loss (D) will reduce as a function of air flow rate. If the air flow is high enough then it is possible for all of the fabric heat loss to be recovered.

Dynamic U-value is a parameter that has been used in the past to quantify heat loss through a dynamically insulated wall. The 'dynamic' in this case stems from the fact that the net fabric heat loss (D) changes as a function of air flow rate.

Dynamic Insulation Theory

Dynamic insulation can take different forms. The two basic types of dynamic insulation that form a part of the Energyflo product range are briefly presented and discussed in this section.

1. Permeodynamic insulation

   With permeodynamic insulation the air flow is through the insulation, normal to the plane of the dynamically insulated wall and counter to the direction of heat flow. The materials from which the insulation is made are air permeable. Figure 2(a) is a schematic representation of a permeodynamic wall.

   The dynamic U-value $U_{d\text{-}ef}$ of a permeodynamic insulation layer within a wall or building envelope element is (M S Imbabi, 2006):

$$U_{d-ef} = \frac{v_a \rho_a C_a}{\exp(v_a \rho_a C_a R_s) - 1} \qquad (1)$$

   Where v_a is the air flow rate per unit area of insulation, ρ_a is the density and C_a the specific heat capacity of air and R_s is the static thermal resistance (R-value) of the dynamic insulation layer in the absence of air flow.

2. Parietodynamic insulation

   Parietodynamic insulation offers an alternative approach where air flow is confined to a channel or channels within the plane of the wall and the direction of flow is orthogonal to the direction of heat flow. The materials used are ideally impermeable to air flow and channels may be enclosed or exposed. Figure 2(b) is a schematic representation of a parietodynamic wall.

   The average dynamic U-value of a parietodynamic insulation layer within a wall or building envelope element is (M S Imbabi et al, *in preparation*):

$$\overline{U}_{d-ch} = \frac{(M - T_o)((e^{-hN} + hN - 1)}{(T_i - T_o) R_o \times hN} \qquad (2)$$

   Where $M = (R_o T_i + R_i T_o)/(R_o + R_i)$, $N = (R_o + R_i)/(\rho_\alpha C_a v_u R_o R_i)$, T_i and T_o are the indoor and outdoor temperatures, h is the wall height, R_o and R_i are the lumped thermal resistances (R-values) between the air flow channel and the cladding to insulation interfaces, ρ_a the density, C_a the specific heat capacity of air and $v_u = v_a h$

is the volumetric air flow rate per unit width of dynamic wall of height h. v_a is the normalised volume flow rate per unit area of dynamic wall.

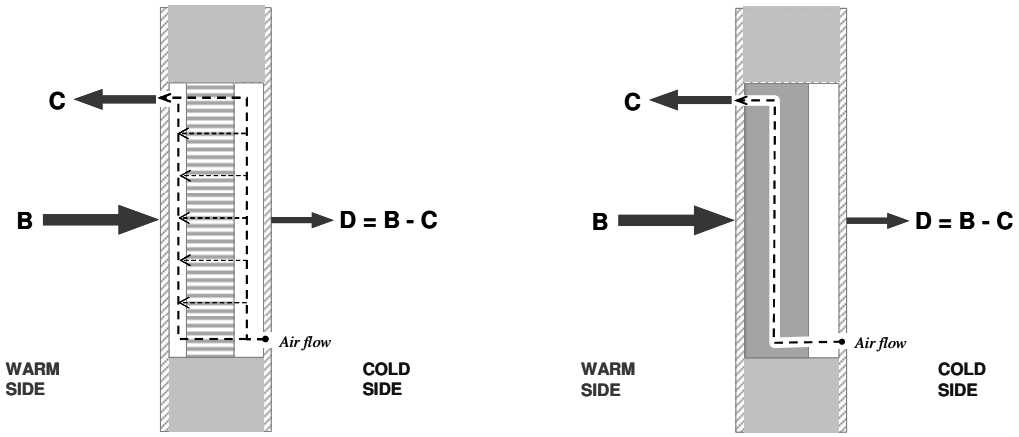

(a) Permeodynamic wall (b) Parietodynamic wall

Figure 2

Eqs (1) and (2) do not cater for radiant or convective heat transfer effects and do not include the thermal mass effects of external and internal cladding materials. They can be used within the standard BS EN ISO 6946 (2007) Calculation Method to work out the overall dynamic U-value of the wall construction under steady state conditions.

In order to model transient response it is necessary to specify a dynamic R-value for the insulation layer on its own, thus permitting the inertial effects of the rest of the wall construction to be represented (if applicable) using whatever approach that the modeler already uses.

The governing equations for each of the permeo and parieto forms of dynamic insulation that have been outlined, including expressions for dynamic R-value and the associated supply air temperature rise as functions of air flow rate, will be introduced in the next section.

Finally, irrespective of whether the construction is permeo or parietodynamic, it will have some 'other' layers in the heat flow path. The total U-value U_t of the envelope element thus contains U_o and U_d contributions as shown in Eq (3).

$$U_t = [U_o^{-1} + U_d^{-1}]^{-1} \quad (3)$$

From the above, as $U_d \rightarrow 0$, the fixed contribution from U_o becomes negligibly small. Assuming $U_t = U_s$ when the air flow is zero, then a normalised (U_t/U_s) can be plotted as a function of the air flow rate for walls employing permeodynamic and parietodynamic insulation. The form of this relationship is shown in Figure 3. In both cases this shows U_t falling as the air flow rate increases. The rate of fall for two types is not the same suggesting the performance of the permeodynamic wall is intrinsically superior to the parietodynamic wall given the same starting U-value. This benefit is countered by the wider range of impermeable materials with low static thermal conductivity that can be used to fabricate the latter. The value of U_s for parietodynamic insulation will thus generally be lower for the same thickness of permeodynamic insulation.

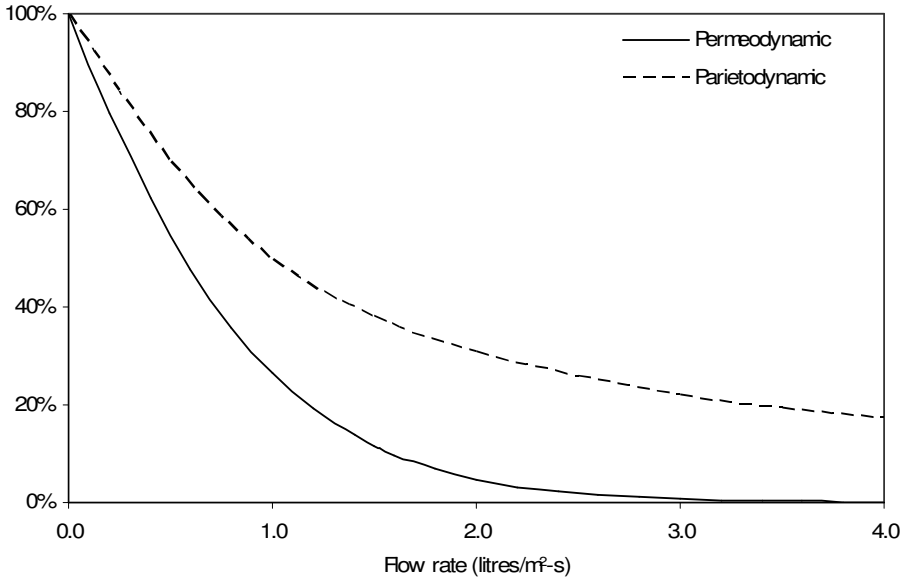

Figure 3. Normalised plots of (U_d/U_s) versus the flow rate v_a

Implementation and Governing Equations

The governing equations used to model the steady-state behaviour of dynamic insulation are presented in this section. These equations have been shown to faithfully represent the heat transfer processes that occur in dynamic insulation. Their accuracy has been proven through modified hot box tests by the National Physical Laboratory (NPL), paving the way for their use with confidence in SAP Appendix Q calculations. Copies of NPL reports PP31/E09040147 and PP31/2010030629 form part of the submission.

3. Permeodynamic equations

The theoretical equations in this section are presented with reference to the figure below (and the notation therein). These are the equations intended for use in SAP Appendix Q calculations. Full derivations of these equations can be found in the accompanying document 'Analytical Model of a Hybrid Permeodynamic Wall'.

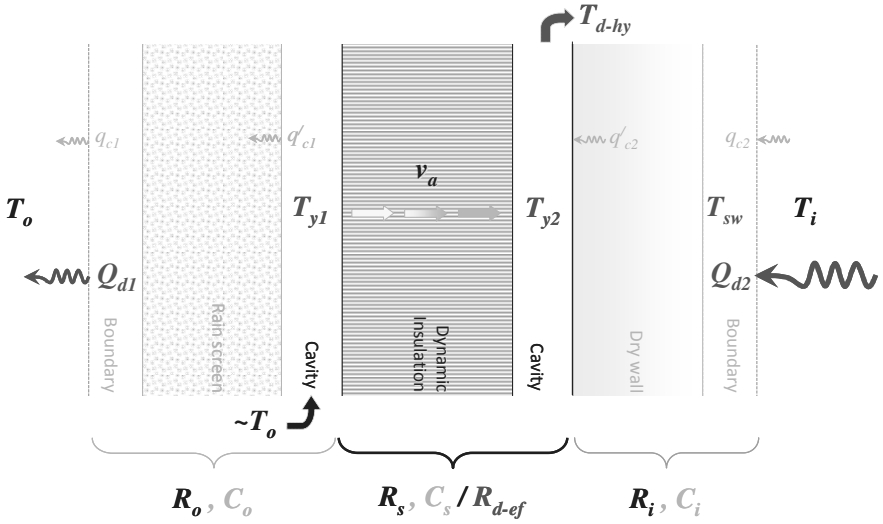

Figure 4

3.1 Steady state heat flux Q_s and internal cavity temperature T_{y2} in static mode.

$$Q_s = U_s \Delta T = \frac{(T_i - T_o)}{(R_o + R_s + R_i)} \tag{4}$$

$$T_{y2} = T_i - Q_s R_i \tag{5}$$

3.2 *Steady-state dynamic R-value $R_{d\text{-}ef}$, external* heat *flux Q_{d1}, dynamic U-value U_{1d}, the external and internal cavity temperatures T_{y1} and T_{y2} and the air supply temperature $T_{d\text{-}ef}$ in dynamic mode.*

From Eq (1), it is evident that:

$$R_{d-ef} = \frac{1}{U_{d-ef}} = \frac{\exp(v_a \rho_a C_a R_s) - 1}{v_a \rho_a C_a} \tag{6}$$

Where again ρ_a and C_a are the density and specific heat capacity of air, and R_s the thermal resistance of dynamic insulation when the air flow rate v_a = 0

$$Q_{1d} = \frac{T_i - T_o}{R_o + R_{d-ef} + R_i} \tag{7}$$

$$U_{1d} = \frac{Q_{1d}}{T_i - T_o} = \frac{1}{R_o + R_{d-ef} + R_i} \tag{8}$$

$$T_{y1} = T_o + \frac{R_o (T_i - T_o)}{R_o + R_{d-ef} + R_i} \tag{9}$$

$$T_{y2}(y) = A + \frac{F^*}{e^{\frac{Cy^2}{2}}} \tag{10}$$

where

$$A = \left[\frac{T_i (R_o + R_{d-ef}) + T_o R_i + \rho_a C_a v_a R_i (R_o + R_{d-ef})(T_{y1} - T_o)}{R_o + R_{d-ef} + R_i} \right] \tag{11}$$

$$C = \left[\frac{\rho_a C_a v_a R_i (R_o + R_{d-ef})}{R_o + R_{d-ef} + R_i} \right] \tag{12}$$

$$F^* = T_{y2}(0) - A = \frac{T_o\left(\rho_a C_a v_a R_i\left(R_o + R_{d-ef}\right) + R_i\right) + T_i\left(R_o + R_{d-ef}\right)}{R_o + R_{d-ef} + R_i + \rho_a C_a v_a R_i\left(R_o + R_{d-ef}\right)} - A \quad (13)$$

The air supply temperature $T_{d\text{-}ef}$ from a dynamic wall of height h may be obtained from Eq (10) at $y = h$. Thus

$$T_{d-ef} = T_{y2}(h) = A + \frac{F^*}{e^{\frac{Ch^2}{2}}} \quad (14)$$

3.3 *Validation of Eqs (8) and (14) against the NPL test results.*

As part of the SAP Appendix Q process, NPL was commissioned by the Building Research Establishment (BRE), to develop an appropriate test method for dynamic insulation, and to apply this method to assess the performance of the Energyflo® EF04 cell.

The results reported in Table 1 were taken from the modified hot box test results reported in accompanying NPL report number PP31/E09040147. The analytical results from the Hybrid Permeodynamic Model (HPM) are presented in Table 2. Figs 5 and 6 enable direct comparisons of Dynamic U-value U_{1d} and air supply temperature $T_{d\text{-}ef}$ across the test range to be made.

Table 1. NPL test results.

Test Number	v_a ***(L/m²/s)***	T_i ***(C)***	T_o ***(C)***	Q_o ***(W)***	$T_{d\text{-}ef}$ ***(C)***	**-**	U_{1d} ***(W/m²K)***
R092A	0.00	22.05	1.86	14.17	n/a	-	0.49
R092V	0.60	21.93	2.00	6.24	20.56	-	0.22
R092L	1.04	21.97	2.00	3.45	20.13	-	0.12
R092N	1.50	21.88	2.07	2.21	19.72	-	0.08
R092M	1.98	21.88	2.07	2.10	19.39	-	0.07
R092J	3.36	21.94	2.01	0.83	18.74	-	0.03

Table 2. Analytical results (HPM)

					Eq (14)	*Eq (8)*	
Test Number	v_a ***(L/m²/s)***	T_i ***(C)***	T_o ***(C)***	h^2Q_{1d} ***(W)***	$T_{d\text{-}ef}$ ***(C)***	U_{1d} ***(W/m²K)***	$U_{1d\text{-}adj}^{(1)}$ ***(W/m²K)***
R092A	0.00	22.05	1.86	14.39	n/a	0.50	0.50
R092V	0.60	21.93	2.00	7.20	20.21	0.25	0.25
R092L	1.04	21.97	2.00	3.96	19.71	0.14	0.14
R092N	1.50	21.88	2.07	1.95	19.11	0.07	0.08
R092M	1.98	21.88	2.07	0.88	18.61	0.03	0.05
R092J	3.36	21.94	2.01	0.07	17.64	0.00	0.03

(1) Adjusted to account for parieto recovery from the solid fraction (see box, page 8)

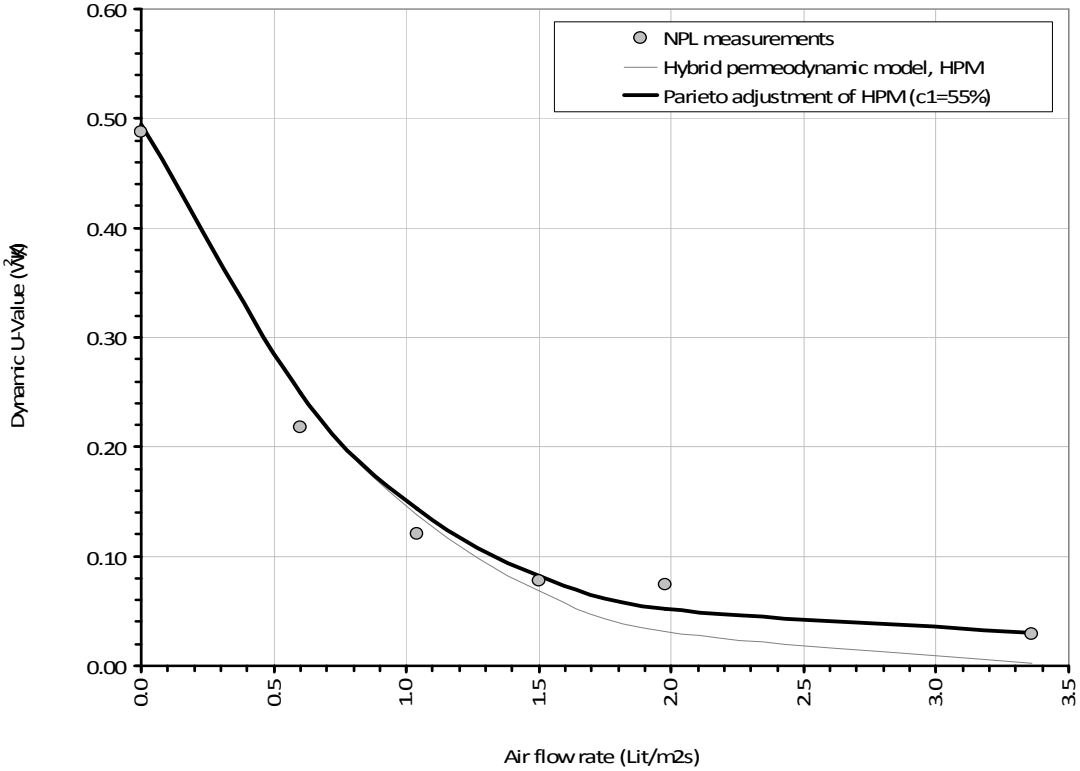

Figure 5. Plot of theoretical vs measured dynamic U-values *vs* air flow rate, NPL EF04 test sample (V).

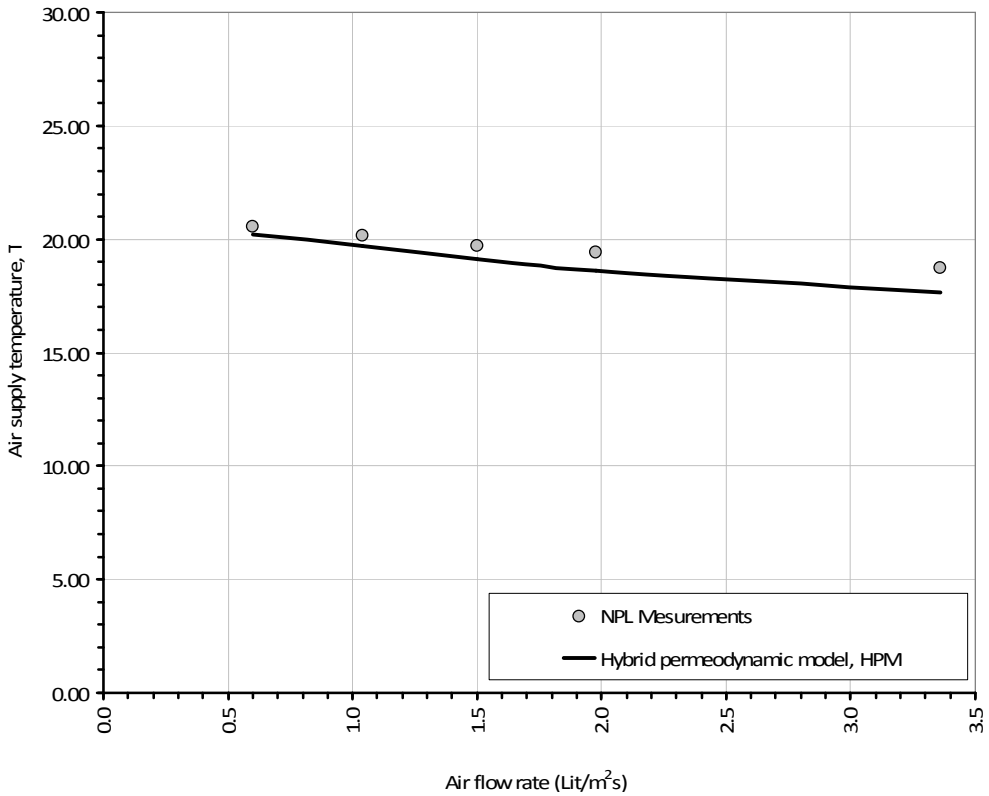

Figure 6. Plot of theoretical vs measured air supply temperatures *vs* air flow rate, NPL EF04 test sample (V).

Parietodynamic correction for EF cells

Not all of the incoming air flows through the cells. Some of it flows across the cell surround, which for the EF04 product is around 31% of the face area. A proportion of the heat loss via this route – 55% fits well – is parieto-dynamically recovered and drawn in through the permeable fraction of the cell.

A_{static} =	31%	from specs
R_{static} =	3.17	from specs
U_{static} =	0.32	= 1 / R_{static}
c1 =	55%	Recovered fraction
c2 =	1.14	= 1 + (1 - c1) x A_{static}

$$U_{dynamic} = [U_{permeo} + U_{parieto}]^{c2}$$

This example assumes thermal bridging across the static fraction of the cell, with 55% of the heat loss recovered parieto-dynamically

$$U_{parieto} = (1 - c1) \times U_{static} \times A_{static}$$

The results that have bee presented provide a level of agreement between NPL laboratory tests and analytical model predictions that is well within the bounds of experimental error, fully validating the theoretical the model.

Adjustment of the predicted dynamic U-value at air flow rates higher than 1.0 Lit/m^2/s, based on considerations of parietodynamic heat recovery from the solid fraction of the test sample and the NPL results, is proposed – see the adjusted U-value curve in Fig 5. The NPL supply air temperatures in Fig 6 show excellent agreement with analytical model predictions obtained using Eq (14).

On the basis of these results, users of the model can estimate the performance of any permeodynamic wall construction, given knowledge of the construction, the materials used, ventilation air flow rate and the local environment.

4. Parietodynamic (channel) equations

The theoretical equations in this section are presented with reference to the figure below (and the notation therein). These are the equations intended for use in SAP Appendix Q calculations. Full derivations of these equations can be found in the accompanying document 'Analytical Model of a Parietodynamic Wall'.

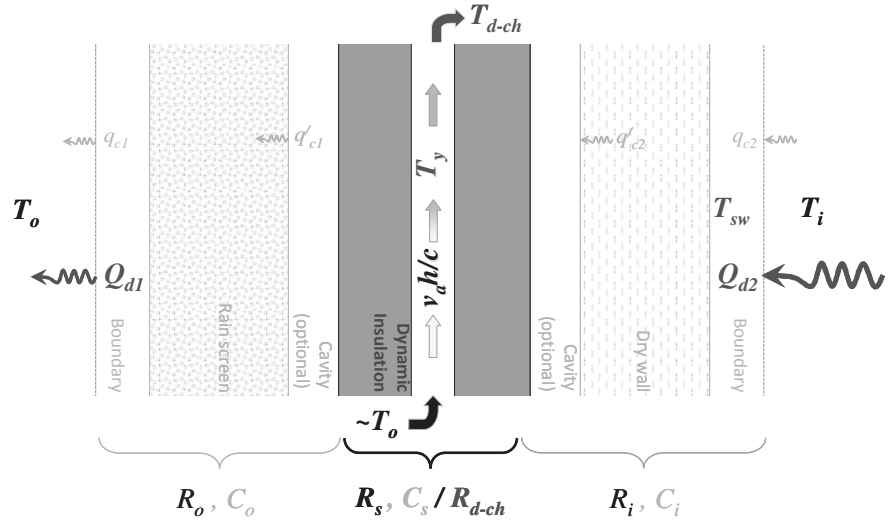

Figure 7

4.1 Steady state heat flux Q_s in static mode.

$$Q_s = U_s \Delta T = \frac{(T_i - T_o)}{(R_o + R_s + R_i)} \qquad (15)$$

where R_s is the static thermal resistance of the cell in the absence of air flow.

4.2 *Steady-state dynamic R-value $R_{d\text{-}ch}$, external heat fluxes Q_{d1}, dynamic U-value U_{1d}, U_{2d} and air supply temperature $T_{d\text{-}ch}$ in dynamic mode.*

From Eq (2), it is evident that:

$$\overline{R}_{d-ch} = \frac{1}{U_{d-ch}} = \frac{(T_i - T_o)(R_o + \alpha R_s) \times hN}{(M - T_o)((e^{-hN} + hN - 1)} \quad (16)$$

where h is the wall height or channel length, α is the outward facing fraction of R_s that lies beyond the channel centre-line (the value of α lies between 0 and 1, and is equal to 0.5 if the channel is located mid-way through the depth of the dynamic insulation layer), and

$$M = ((R_o + \alpha R_s)Ti + (R_i + (1-\alpha)R_s)T_o)/(R_o + R_s + R_i) \quad (17)$$

$$N = (R_o + R_s + R_i)/((R_o + \alpha R_s)(R_i + (1-\alpha)R_s))v_u \rho_a c_a) \quad (18)$$

$$\overline{Q}_{d1} = \frac{(M - T_o) \times (e^{-hN} + hN - 1)}{hN(R_o + \alpha R_s)} \quad (19)$$

$$U_{1d} = \frac{Q_{1d}}{T_i - T_o} = \frac{(M - T_o) \times \left(e^{-hN} + hN - 1\right)}{hN(R_o + \alpha R_s)(T_i - T_o)} \quad (20)$$

$$T_y(y) = M + (T_o - M) \times e^{-Ny} \quad (21)$$

The air supply temperature $T_{d\text{-}ch}$ from a dynamic wall of height h may be obtained from Eq (21) at $y = h$. Thus

$$T_{y-ch}(h) = M + (T_o - M) \times e^{-Nh} \quad (22)$$

4.3 *Validation of Eqs (20) and (22) against the NPL test results.*

In accordance with the process outlines in section 3.3 and using the same test methods, NPL was commissioned to test a prototype parietodynamic insulation product, the XStream XS01.

The results reported in Table 3 were taken directly from the modified hot box test results reported in the accompanying NPL report number PP31/2010030629. The analytical results from the parietodynamic model are presented in Table 4. Figs 8 and 9 against the experimentally derived dynamic U-value U_{1d} and air supply temperature $T_{d\text{-}ch}$ and show good agreement. As before, adjustment of predicted dynamic U-values, based on considerations of parietodynamic heat recovery from the solid fraction of the cell and the observed trend in the NPL results, has been applied to derivation of the adjusted dynamic U-value curve in Fig 8.

Table 3. NPL test results.

Test Number	v_a *(L/m²/s)*	T_i *(C)*	T_o *(C)*	Q_i *(W)*	Q_o *(W)*	$T_{d\text{-}ch}$ *(C)*	U_{1d} *(W/m²K)*
R105A	0.00	22.25	2.14	8.95	8.95	-	0.31
R105D	0.28	22.10	2.10	11.40	7.30	12.24	0.25
R105C	0.71	22.17	2.15	13.94	4.77	10.23	0.16
R105B	1.25	22.21	2.23	15.66	3.42	8.51	0.12

Table 4. Analytical results (PAR)

				Eq (22)		*Eq (20)*	
Test Number	v_a *(L/m²/s)*	T_i *(C)*	T_o *(C)*	h^2Q_{1d} *(W)*	h^2Q_{1d} *(W)*	$T_{d\text{-}ch}$ *(C)*	U_{1d} (1) *(W/m²K)*
R105A	0.00	22.25	2.14	8.97	8.96	-	0.31
R105D	0.28	22.10	2.10	11.29	6.11	11.84	0.22
R105C	0.71	22.17	2.15	13.65	4.02	9.79	0.15
R105B	1.25	22.21	2.23	14.99	2.74	7.81	0.11

(1) Adjusted to account for parieto recovery from the solid fraction (see box, page 8)

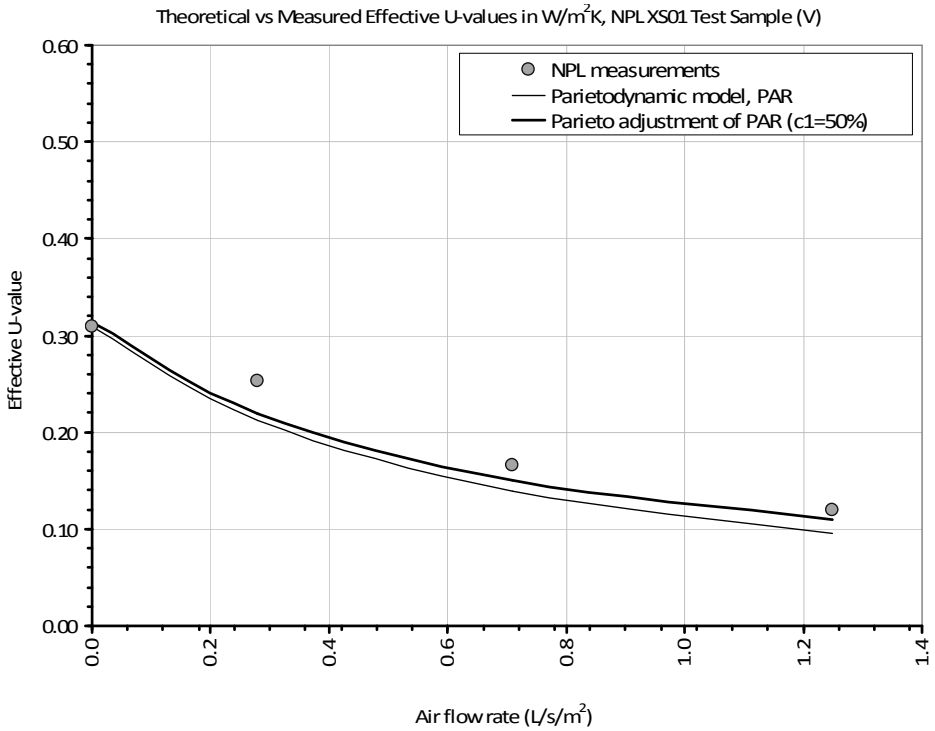

Figure 8. Plot of theoretical vs measured dynamic U-values *vs* air flow rate, NPL XS01 test sample (V)

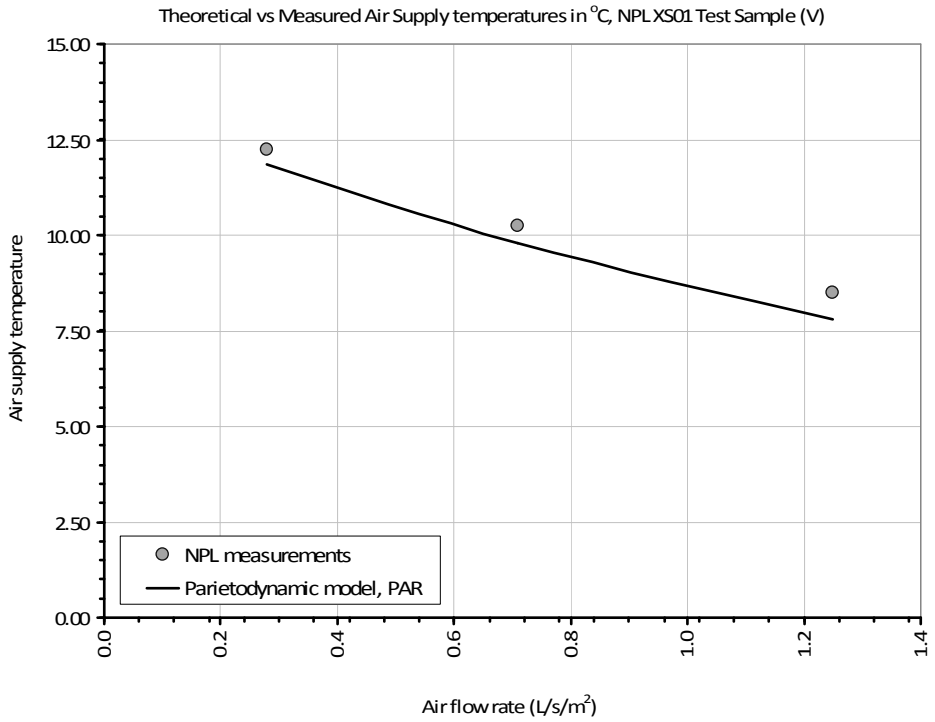

Figure 9. Plot of theoretical vs measured air supply temperatures *vs* air flow rate, NPL XS01 test sample (V)

5. Design air flow rate

The previous sections show how the steady-state performance of dynamic insulation can be modeled theoretically. The static R-value, R_s, and in the case of parietodynamic insulation the height h and the fraction of insulation material between the channel and the external rain screen cladding. α,, are the inputs that, together with the air flow rate v_a, substantially define the dynamic insulation effect.

Irrespective of the type of dynamic insulation that is being considered, the air flow rate is most conveniently expressed as a volume flow rate unit area of dynamic insulation. In SI units, v_a may be conveniently expressed in m^3/m^2s, or $litres/m^2s$. Experience shows that the latter units are more easily accessible when the building design is being optimised to deliver a specified number of litres/s based on occupancy – i.e., in the majority of cases.

One approach to selecting a design value for v_a to iterate around is to start with a target value, say for example 1 $litre/m^2s$, that can be used to work out the area of the envelope to be dynamically insulated for a given air change rate – i.e.,

$$Dynamic\ Insulation\ Area\ (m^2) = \frac{Ventilation\ \ Rate\ \ (litres/s)}{v_a\ \ (litres/m^2 s)} \qquad (23)$$

Alternatively, the value of v_a can be determined in from the above equation if the ventilation rate and area of wall that is dynamically insulated are known apriori.

References and Bibliography

Annex 44 A3. Dynamic Insulation. Annex 44 State-of-the-Art Working Report Pt. A3 (2006).

Baker, P H and M McEvoy, Test cell analysis of the use of a supply air window as a passive solar component, Solar Energy Vol. 69(2), p113–130 (2000).

Bartussek H, Poren-luftung (Porous ceilings). Osterreichisches Kuratorium fur Landtechnik, Vienna (1981).

Brown, A R, M S Imbabi and A D Peacock, The transforming technology of dynamic breathing building, Ecocity World Summit 2008, San Francisco (USA). April 24th – 26th 2008.

Dalehaug A, Dynamic insulation in walls. Research report No 53, ISSN 0915-9215, Hokkaido prefectural cold region housing and urban research institute, Japan (1993).

Dimoudi A, A. Androutsopoulos, S. Lykoudis, Experimental work on a linked dynamic and ventilated wall component, Energy and Buildings 36, p443– 453 (2004).

Elsarrag, E, M. Aboulnaga, A. Peacock and M. S. Imbabi, Dynamic insulation for energy conservation and improved indoor air quality in hot humid climates, Invited keynote paper, ASHRAE 5th Chapter Regional Conference (CRC), Dubai (2006).

Elsarrag, E and M S Imbabi. Evaluation of dynamic insulation for zone ventilation and air conditioning in the gulf region. ASHRAE Symposium on Sustrainability and Green Building, Kuwait (2009).

Imbabi M S, and A Peacock, Smart breathing walls for integrated ventilation, heat exchange, energy efficiency and air filtration. ASHRAE/CIBSE conference, Edinburgh (2003).

Imbabi M S, and A D Peacock, Allowing buildings to breathe, Sovereign Publications (2004).

Imbabi M S, Modular breathing panels for energy efficient, healthy building construction, Renewable Energy, Vol. 31, Issue 5, p 729-738 (2006).

Imbabi M S, Full-scale evaluation of energy use and emissions reduction of a dynamic breathing building, Proceedings of WREC-IX, Florence, 19-25 August (2006).

Imbabi, M S, The performance of dynamic breathing buildings in the United Arab Emirates, Invited keynote paper, Environment 2007 Conference, Abu Dhabi (2007).

Imbabi, M S, E Elsarrag and A R Brown, Heat transfer in parietodynamic insulation, *in preparation* (2010)

Straube, J F and V Acahrya, Indoor air quality, healthy buildings, and breathing walls, Building Engineering Group, Civil Engineering Department, University of Waterloo, Ontario (2000).

Taylor, B J, D A Cawthorne and M S Imbabi, Analytical investigation of the steady-state behavior of dynamic and diffusive building envelopes, Building and Environment, Vol. 31(6), p519-525 (1996).

Taylor B J, and M S Imbabi, The effect of air film thermal resistance on the behavior of dynamic insulation, Building & Environment, Vol. 32(5), p397-404 (1997).

Taylor B J, R Webster and M S Imbabi, The building envelope as an air filter, Building & Environment, Vol. 34(3), p353-361 (1998).

Taylor B J and M S Imbabi, Dynamic insulation in multi-storey buildings, Proc. CIBSE A, Building Services Engineering Research & Technology (BSERT), 20(4), p175-180 (2000).

Taylor B J and M S Imbabi, Environmental design using dynamic insulation, ASHRAE Transactions, Vol. 106(1), p15-28 (2000).

Wallenten P, OPTIMAT field measurements of dynamic insulation. Proceedings of the 3rd Symposium Building Physics in Nordic Countries, Vol. 1, p243-251, Copenhagen, 13-15 September (1993).

Wong J M, F P Glasser, and M S Imbabi, Breathable concrete for low energy buildings, Proceedings of WREC2005, 22-27 May (2005).